

Sugar-Based Thermoplastic Polyhydroxyurethanes: Effects of Sorbitol and Mannitol Diastereomers on Polymer Properties and Applications in Melt Blending

Georges R. Younes, Marc Kamel, Hatem M. Titi, Mohammad Farkhondehnia, and Milan Marić*

Cite This: *ACS Appl. Polym. Mater.* 2022, 4, 5161–5172

Read Online

ACCESS |



Metrics & More

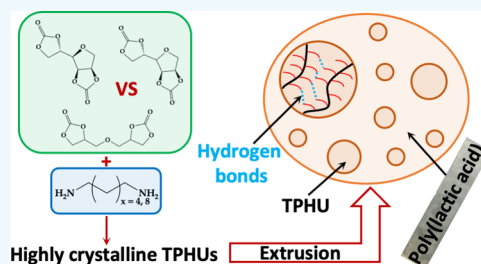


Article Recommendations



Supporting Information

ABSTRACT: Each of the three bio-sourced dicarbonates, sorbitol biscarbonate (SBC), mannitol biscarbonate (MBC), and diglycerol dicarbonate (DGC), is polymerized with 1,6-hexamethylenediamine (HMDA) or 1,10-diaminodecane (DAD) in dimethyl sulfoxide for 24 h at 100 °C to obtain highly crystalline (70–77%) thermoplastic polyhydroxyurethanes (TPHUs). Even though SBC and MBC are isomers, their respective TPHUs present similar (micro)structural, thermal, and rheological properties. However, MBC reacts faster with amines at room temperature and induces more flexibility into the TPHU chains than SBC. The glass transition temperatures (T_g s) of the MBC-based TPHUs are 7 °C lower than those of the SBC-based ones. Interestingly, the HMDA-based TPHUs exhibit liquid crystalline-like rheological behavior with their storage moduli increasing above their apparent melting points. Nevertheless, replacing SBC and MBC, whose structure contains a rigid furan ring, by DGC, a linear aliphatic dicarbonate, significantly alters the properties of the TPHUs, especially the rheological ones. The storage modulus of the DGC-DAD TPHU is ten-fold lower than those of the SBC and MBC analogues, when measured at similar conditions. MBC-HMDA, MBC-DAD, and DGC-DAD are then blended into poly(lactic acid) (PLA) (20/80 wt%/wt%), and the blends are predicted to be miscible from the Hoftyzer–Van Krevelen group contribution method. While PLA/MBC-HMDA and PLA/MBC-DAD show one T_g , the PLA/DGC-DAD presents two, despite the predicted miscibility of that blend. However, both T_g s are shifted lower compared to the homopolymers, indicating that the components of that blend act as plasticizers of a two-phase morphology, as implied by droplets no more than 5 μm in diameter in the PLA matrix observed from SEM. Despite their miscibility with PLA, the TPHUs agglomerate into droplets inside the blends caused by significant intramolecular hydrogen bonding interactions between their chains. These results expand the application of TPHUs as nontoxic additives, for example, plasticizers, reinforcing agents, rubber tougheners, and composites into different polymer matrices.



KEYWORDS: sugars, polyhydroxyurethanes, polymer blending, group contribution method, crystalline polymers

INTRODUCTION

Nonisocyanate polyurethanes (NIPUs) have been greatly investigated in the last decade because they do not contain isocyanates, a toxic main component of conventional polyurethanes (PUs).^{1,2} One of the NIPU routes involves the polyaddition of cyclic (poly)carbonates with (poly)amines, and it leads to polymeric materials with pendent hydroxyl groups, known as polyhydroxyurethanes (PHUs). The PHU route is prominent because the polymerization does not form lower molecular weight byproducts and the monomers are abundant and, most importantly, they can be bio-sourced.^{2–4} Actually, cyclic carbonates were previously synthesized from vegetable oils, bio-polyols (sugars and glycerol), and terpenes,^{5–7} while diamines were obtained from plant-based fatty acids.^{8–10} Interestingly, researchers also took advantage of the chemical fixation reaction of carbon dioxide to prepare different cyclic carbonates from petrochemical and natural sources.¹¹

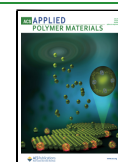
Two notable renewable sources for making cyclic carbonates are diglycerol and diastereomeric D-sorbitol and D-mannitol sugars. Diglycerol dicarbonate (DGC) is derived from glycerol,

which is a byproduct obtained from the hydrolysis of biomass wastes, the methanolysis of triglycerides, and the production of biodiesel, whereas sorbitol and mannitol biscarbonates (SBC and MBC, respectively) are acquired from sugars obtained from glucose processing.⁴ While DGC was extensively explored in the literature for different PHU formulations,^{12–26} SBC and MBC were not,^{27–30} and that could be related to the low melting point of DGC (65 °C),^{12,13} which allows it to react with diamines in bulk and at moderate conditions, compared to the high melting points of SBC and MBC (214–216 °C and 181–183 °C, respectively).²⁷

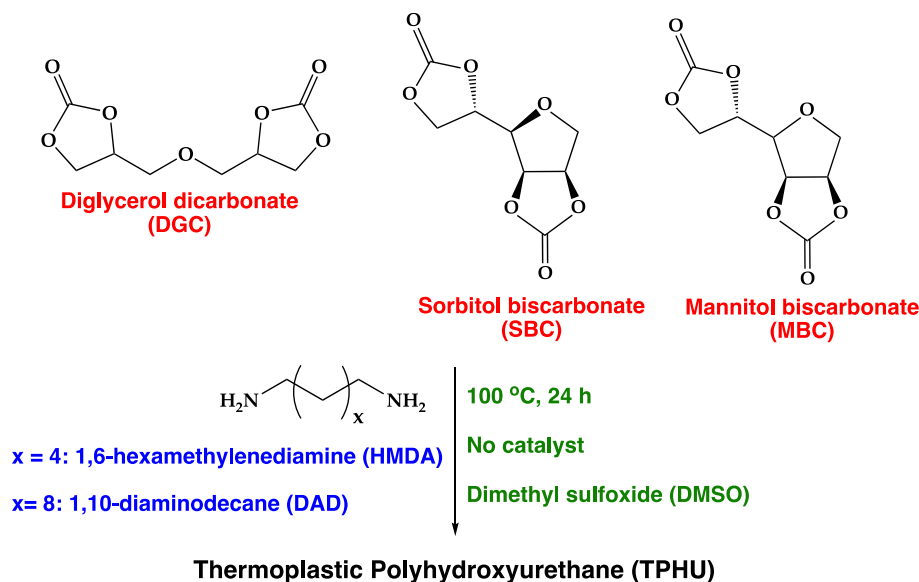
Received: April 19, 2022

Accepted: June 14, 2022

Published: June 28, 2022



Scheme 1. Polyaddition Reaction of the Bio-Sourced Cyclic Dicarbonates of This Work with Different Diamines



In this study, the effect of changing the dicarbonate structure on the properties of the final thermoplastic PHUs (TPHUs) is investigated. Because both sugar-derived dicarbonates are diastereomers, it is anticipated that they will affect differently the properties of their respective TPHUs. A comparison between the TPHUs prepared from SBC/MBC dicarbonates containing a furan ring and DGC, a linear aliphatic dicarbonate, is also conducted. To achieve this goal, low molecular weight diamine soft segments are used: 1,6-hexamethylenediamine (HMDA) and 1,10-diaminodecane (DAD). Also, solution polymerizations are conducted in dimethyl sulfoxide (DMSO) to eliminate the variation caused by the difference of the dicarbonates' melting points while ensuring good mixing of the monomers and high conversions. While bio-based TPHUs have been extensively studied in the literature,^{31–38} a similar approach was adopted by a few, such as Beniah et al., who explored the effects of the choice of dicarbonates on tuning the nanophase separations of their TPHUs prepared from poly(tetramethylene oxide)-based diamines.³⁹ The monomers as well as the reaction pathway followed in this work are presented in Scheme 1.

Moreover, our group recently examined the application of TPHUs in melt blending with poly(lactic acid) (PLA), which is a biopolymer with outstanding physical and mechanical properties but poor ductility and impact toughness.²⁵ While many thermoplastic PUs (TPUs) were extruded with PLA with the intention to plasticize the latter and increase its toughness and ductility,^{40–52} our study was the first, to our knowledge, to investigate TPHUs for a similar application.²⁵ We found that the DGC-based TPHUs were partially miscible with PLA, and some of them exhibited plasticization and/or toughening of the PLA matrix because of hydrogen bonding interactions in the blends. Using TPHUs as additives is an interesting application because high molecular weight PHUs are difficult to obtain, as side products limit the polyaddition of dicarbonates and diamines.⁵³

To complement our previous results and to achieve better miscibility with PLA, this work also examines the blending of the synthesized TPHUs with PLA and uses the Hoftyzer–Van Krevelen group contribution method to predict and confirm

the experimental results.⁵⁴ We speculate that because shorter diamines are used here compared to our previous study and higher molecular weights of the TPHUs are achieved (more hydroxyl groups present per chain), we could potentially increase the number of TPHU/PLA hydrogen bonding interactions.²⁵

Briefly, this study starts by examining the effects of the dicarbonates (SBC, MBC, and DGC) on the TPHU properties. The resulting TPHU's (micro)structural, thermal, and rheological properties are studied and compared. Then, the blends of PLA with the TPHUs are prepared and characterized in terms of miscibility, and the experimental results are compared to theoretical predictions from group contribution methods. Finally, insights into the design of TPHU additives to different polymer matrices will be presented.

MATERIALS AND METHODS

Materials. Diglycerol (DIG, $\geq 80\%$ α,α , impurities consist of mono-, α,β -di-, β,β -di, and triglycerol) was obtained from Tokyo Chemical Industry (TCI). D-Sorbitol ($\geq 98\%$ powder), D-mannitol ($\geq 98\%$ powder), 1,5,7,5-triazabicyclo[4.4.0]dec-5-ene (TBD, 98%), 1,6-hexamethylenediamine (HMDA), 1,10-diaminodecane (DAD), 1-octylamine (99%), and deuterated dimethyl sulfoxide (DMSO- d_6) were provided by Sigma Aldrich. Dimethyl carbonate and potassium carbonate (K_2CO_3 , 98%, anhydrous powder) were purchased from Acros. Ethyl acetate (EthOAc, certified grade), dimethyl sulfoxide (DMSO), and chloroform (stabilized with ethanol) were purchased from Fisher Chemical. Water purified using a reverse osmosis process was provided by the McGill Chemical Engineering Department. Poly(lactic acid) (PLA) was purchased from NatureWorks (Product ID Ingeo Biopolymer 2003D). All the chemicals were used as received. Only PLA was dried overnight under vacuum at 40 °C before extrusion to remove any adsorbed moisture.

Experimental Methods. *Dicarbonates Synthesis and Purification.* The synthesis and purification of SBC, MBC, and DGC were conducted following the procedure detailed in previous studies.^{21,30} The SBC, MBC, and DGC yields were 40, 60, and 58%, respectively, based on the total amount of bio-sourced raw materials originally loaded. The detailed characterization of the $^1\text{H-NMR}$ and Fourier transform infrared (FT-IR) spectra of the cyclic dicarbonates can be found elsewhere.^{21,30}

Kinetic Study of SBC and MBC. The reactivity of the SBC and MBC during the aminolysis reaction was assessed by reacting each of the sugar-based dicarbonates with 1-octylamine using equimolar functionality of cyclic carbonates and amines. The bulk reaction was allowed to proceed at room temperature (~ 22 °C) until a solid compound was formed. Room temperature was selected because erythritol dicarbonate, which is also sugar-derived, was observed to be fairly reactive at room temperature.³¹ The reactions with SBC and MBC were stopped after 115 and 25 min, respectively.

Thermoplastic PHU Synthesis. The PHUs were synthesized through solution/stoichiometric polyaddition of the monomers. The cyclic dicarbonate (SBC, MBC, or DGC) and the diamine (HMDA or DAD) were dissolved and mixed in DMSO at a concentration of 1 mol/L in a 100 mL reactor. After adding a high viscosity stir bar into the mixture, the contents were purged with nitrogen for 15 min before immersing the reactor in an oil bath preheated to 100 °C. The reaction was allowed to proceed for 24 h, after which the reactor was removed from the oil bath to cool down, and water was added to precipitate the TPHU. Using vacuum filtration, the TPHU was collected and dried in a vacuum oven at 40 °C for 48 h. The resulting TPHU were named based on the cyclic dicarbonate (CC) and the diamine (DA) used to prepare them, such that the nomenclature appears as CC-DA (where CC = SBC, MBC, or DGC while DA = HMDA or DAD).

Extrusion. PLA was blended with some of the TPHUs (MBC-HMDA, MBC-DAD, and DGC-DAD) using a conical intermeshing twin-screw extruder (Haake Minilab, Thermo Electron Corporation, Beverly, MA, USA) with a screw diameter of 5/14 mm in the conical section, a screw length of 109.5 mm, and two batches equal to 3 g each. A three-step process was used to ensure homogeneity of the blends. In the first step, PLA was combined with 20 wt% TPHU to make a batch of 3 g, and the extruder was set at 150 °C with a screw rotation speed of 30 min⁻¹, and the resulting blend was recycled through the extruder with an additional 1.5 g of the mixture for a second step and then for a third one to ensure that the polymers were well mixed. The concentration of 20 wt% was chosen to reflect a typical amount of plasticizer that is used industrially.

Characterization Methods. Proton Nuclear Magnetic Resonance (¹H-NMR) Spectroscopy. Solution-phase NMR spectra were recorded on a Bruker 500 MHz instrument (16 scans) at ambient temperature. The TPHUs were dissolved in DMSO-*d*₆ to be analyzed.

Fourier Transform Infrared (FTIR) Spectroscopy. FTIR measurements were carried out on a Perkin Elmer instrument (Spectrum II series) equipped with a single bounce diamond attenuated transmission reflectance (ATR) for solids and zinc selenide (ZnSe) holder for liquids. 32 scans were recorded for each sample over the range 4000–500 cm⁻¹ with a normal resolution of 4 cm⁻¹. The TPHUs and the samples resulting from the kinetic study were measured as is, whereas the blends were solvent cast from chloroform.

Thermogravimetric Analysis (TGA). TGA was performed on a Q500 system from TA Instruments. The thermal degradation of the synthesized TPHU and the cyclic dicarbonates was measured at a heating rate of 20 °C/min over the temperature range of 25–600 °C under a nitrogen atmosphere. The 10 and 50% degradation temperatures ($T_{d,10\%}$ and $T_{d,50\%}$) were calculated using this method.

Differential Scanning Calorimetry (DSC). DSC was performed using a Q2500 TA Instruments calorimeter autosampler employing standard hermetic aluminum pans, calibrated with indium and nitrogen as purge gas. The instrument is equipped with a cooling unit allowing it to reach low temperatures up to -90 °C. The samples were analyzed at a heating rate of 10 °C/min, for the second heating ramp, over a temperature range of -90 to 180 °C or -25 to 180 °C for the TPHUs or the PLA/TPHU blends, respectively, under a nitrogen atmosphere. Glass transition temperatures (T_g), crystallization temperatures (T_c), melting points (T_m), and the associated enthalpies with the crystallization and the melting (ΔH_c and ΔH_m , respectively) were calculated from the second heating ramp.

Small- and Wide-Angle X-Ray Scattering. Small-angle X-ray scattering (SAXS) and wide-angle X-ray scattering (WAXS) measurements were recorded on a SAXSpoint 2.0 (Anton Paar, Austria)

equipped with a CuK α radiation source (wavelength, $\lambda = 1.54$ Å), using a detector (Eiger R 1 M (Horizontal)) at SAXS and WAXS distances of 1075.9 and 113.1 mm, respectively. The TPHU samples, with a thickness of 1 mm, were placed on a sample holder for solids (10 by 10 mm) provided by Anton Paar, which was further secured by tape. X-ray exposure times were 30 min per frame for a total of 4 frames for every experiment. The obtained SAXS profiles were corrected and shown as a function of the scattering vector ($q = (4\pi/\lambda) \sin\theta$, where 2θ is the scattering angle in ° and q in nm⁻¹). The mean interdomain spacing, d (nm), was calculated from the obtained SAXS spectra using the following formula:

$$d = \frac{2\pi}{q_{\max}} \quad (1)$$

with q_{\max} (nm⁻¹) is the value of q at the maximum peak position read from SAXS spectra.

The WAXS spectra were replicated using the method of powder X-ray diffraction (XRD) to quantify the crystallinity of the TPHUs using the DIFFRACT.EVA V.4.1 software.

Rheology. For all the rheology tests, TPHU samples were hot-pressed into disks of 25 mm diameter and a thickness of 1–2 mm. The pressing was performed with a Carver hydraulic unit model #3925 at 100 °C for the HMDA-based TPHUs and at 140 °C for the DAD-based TPHUs using three cycles of 5, 10, and 15 metric tons for 10 min each. The temperatures were chosen based on the obtained DSC results.

Amplitude sweep measurements and dynamic mechanical thermal analyses were conducted on the TPHU samples using the 25 mm diameter parallel plate configuration (PP25 with gap 1–2 mm) on an Anton Paar Instruments rheometer (MCR 302). Amplitude sweep measurements were all conducted at room temperature (~ 22 °C) and 150 °C at a frequency of 1 Hz and a shear strain ranging from 0.001 to 1%. The measurements at 150 °C were conducted under nitrogen and using a CTD 450 convection oven, like the DMTA measurements. The latter were performed from 25 to 170 °C at a rate of 5 °C/min, with an oscillation strain of 0.01% and a frequency of 1 Hz, which ensured that the experiments were conducted in the viscoelastic region.

Scanning Electron Microscopy. The morphology of the prepared blends was studied with a Hitachi SU-3500 Variable Pressure SEM instrument using a 10 kV accelerating voltage. The samples were immersed in liquid nitrogen for 10 min before brittle fracture. The surfaces of blend samples were directly treated with DMSO for 5 min to selectively dissolve the TPHUs while keeping the PLA matrix intact, to provide contrast between the two components. The samples then were glued onto the SEM stubs. It should be noted that PLA has low solubility in DMSO at room temperature, enabling its resistance to etching.⁵⁵ The fractured surfaces were imaged after sputter-coating them with a 7 nm coating of platinum (Pt).

RESULTS AND DISCUSSION

Differences between SBC and MBC. Because SBC and MBC are isomeric compounds, they exhibited differences at the structural level, with their ¹H-NMR and FT-IR spectra presenting distinct couplings and fingerprint regions, respectively,³⁰ and in their thermal properties showing a difference of 30 °C in their melting points.²⁷ The difference lies in the spatial orientation in one of the bonds of their furan rings, as it was previously deduced,^{27,30} and that seems to have an impact on the heat resistance of the diastereomers, as SBC has a higher melting point (214–216 °C) than that of MBC (181–183 °C) with the latter revealing partial thermal degradation that starts at 120 °C. Hence, the 10% degradation temperature of MBC was found to be lower than that of SBC (216 versus 276 °C), as shown in Figure S1 of the Supporting Information. Moreover, that difference in strength, brought by the furan ring, affects the reactivity of the sugar-based dicarbonates as well. Indeed, a kinetic study of the bulk aminolysis reaction of

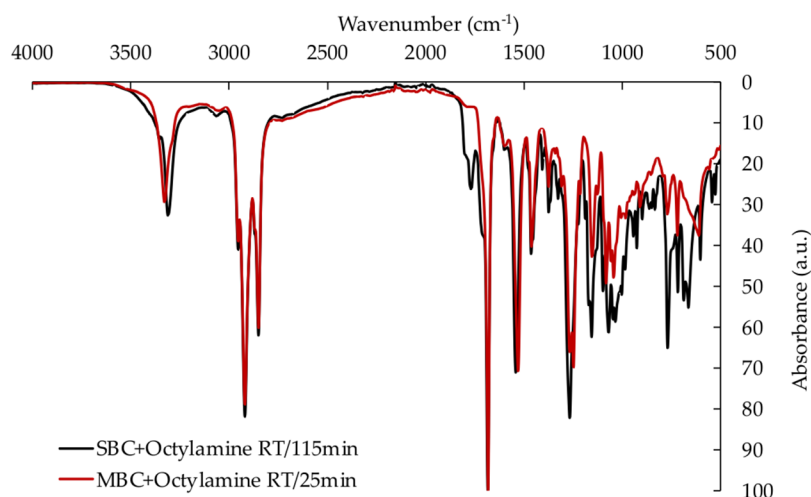


Figure 1. FT-IR spectra showing the complete disappearance of the carbonyl stretch at 1770 cm^{-1} of the cyclic carbonates of MBC and the persistence of that of SBC. With the aminolysis reaction proceeding, the carbonyl stretch at 1770 cm^{-1} was replaced by that at 1685 cm^{-1} , an indication of the formation of urethane linkages.

Table 1. Structural and Microstructural Properties of the Bio-Based TPHUs

| TPHU | p (%) ^a | M_n (g/mol) ^a | $D = M_w/M_n$ ^a | secOH/primOH ^a | X (%) ^b | d (nm) ^c |
|----------|----------------------|----------------------------|----------------------------|---------------------------|----------------------|-----------------------|
| SBC-HMDA | | | | 81/19 | 76 | 4.5 |
| SBC-DAD | | | | 84/16 | 76 | 4.3 |
| MBC-HMDA | 99 | 34,300 | 1.99 | 84/16 | 77 | 7.6 |
| MBC-DAD | 98 | 22,400 | 1.98 | 86/14 | 77 | 4.4 |
| DGC-DAD | 99 | 39,000 | 1.99 | 71/29 | 70 | 2.0 |

^aThe number average molecular weight, M_n , the dispersity, D , the conversion, p , and the percentage of secondary to primary hydroxyl groups are calculated from $^1\text{H-NMR}$ (more information provided in Section II of the Supporting Information). ^bThe crystallinity was calculated from powder XRD. ^cThe interdomain spacing (d) was calculated from eq 1. The value calculated for MBC-HMDA was based on the first q_{max} observed from its SAXS spectrum.

SBC and MBC with 1-octylamine revealed that MBC is more reactive than SBC at room temperature, and its carbonyl stretch at 1770 cm^{-1} disappeared in 25 min as a result of the reaction between the cyclic carbonates with the amines, proven by the presence of the carbonyl stretch of the urethane linkage (amide group) at 1685 cm^{-1} in the FT-IR spectra of Figure 1. The carbonyl stretch of SBC carbonates, on the other hand, persisted even after 115 min, showing that there were still cyclic carbonate groups remaining. This is interesting because MBC could be eventually used in reactive extrusion similarly to DGC and erythritol dicarbonate, another sugar-derived dicarbonate with a high melting point of $169\text{ }^\circ\text{C}$ and good reactivity at room temperature with amines.^{17,31} Similar to MBC and erythritol dicarbonate, it was observed by Schmidt et al. that sorbitol tricarboxylate, a crystalline solid melting at $230\text{ }^\circ\text{C}$, reacted with amines at ambient temperatures; hence, the authors were able to obtain PHU thermosets at moderate conditions despite the high melting point of the tricarboxylate.⁵⁶

Besides, it was seen that the furan ring of SBC and MBC has a positive impact on the strength and the heat resistance of these dicarbonates when compared to DGC, which is a linear aliphatic dicarbonate. In fact, DGC has a low melting point of $65\text{ }^\circ\text{C}$,¹³ and it is less thermally stable than both MBC and SBC, even though MBC partially degrades at low temperatures. The TGA traces of Figure S1 reveal that while DGC has a $T_{d,10\%}$ of $227\text{ }^\circ\text{C}$, it degrades quicker than MBC after $237\text{ }^\circ\text{C}$. These differences observed at the cyclic dicarbonate level triggers many questions about the effects that these monomers will have on the final properties of their respective TPHUs.

These questions are answered in the following sections starting with a detailed comparison between the properties of the sugar-based TPHUs.

Characterization of Sugar-Based TPHUs. The polymerizations were conducted in DMSO to ensure high monomer conversions, and hence, high molecular weights of the TPHUs were achieved. HMDA and DAD are used as the diamines, so the effects of the cyclic dicarbonates is better detected. The FT-IR spectra shown in Figure S2 confirmed the formation of urethane linkages through the presence of carbonyl stretches at 1685 and 1610 cm^{-1} . Multiple carbonyl stretches of the amide groups are present because, during the polyadditions, the cyclic carbonates rings of the nonsymmetric SBC and MBC open in two ways, leading to four different forms of urethane segments, as discussed elsewhere.^{28,30} These four different forms were partially quantified using $^1\text{H-NMR}$, from which the average molecular weights of the TPHUs (number average molecular weight, M_n , and dispersity, D), the conversions of the monomers (p) and the percentage of secondary to primary hydroxyl groups (secOH/primOH) were also estimated. $^1\text{H-NMR}$ was used for molecular weight calculations, relying on the end-group analysis of amines as explained in the Supporting Information, rather than SEC techniques, because the hydroxyl groups in the TPHU chains exhibited high hydrogen bonding interactions, which made the TPHUs poorly soluble in organic solvents, a result observed in erythritol/short diamine-based TPHUs synthesized under similar conditions as in this work.³¹ These interactions are depicted in the FT-IR spectra shown in Figure S2, which

showed a broad and strong band between 3600 and 3000 cm^{-1} of the hydroxyl groups, an indication of the intermolecular bonds of the TPHU chains with each other. The parameters predicted from $^1\text{H-NMR}$ are shown in Table 1, and details on the calculations of these parameters are provided in the $^1\text{H-NMR}$ subsection of Section II of the Supporting Information (Figures S3, S4, and Table S1). The results of p , M_n , and \mathcal{D} drawn from $^1\text{H-NMR}$ are in accordance with the values reported for TPHUs synthesized from erythritol dicarbonates and short-chain diamines under similar reaction conditions,³¹ and the secOH/primOH values are in agreement with values found elsewhere for SBC-based PHUs (between 88/12 and 80/20).²⁹ However, it seems that the aminolysis reaction of MBC tends to form hydroxyurethane linkages containing a slightly higher concentration of secondary hydroxyl groups. It should be noted that the molecular weight results are not reported for the SBC-based TPHUs because the protons adjacent to unreacted amine end groups could not be confidently identified in the $^1\text{H-NMR}$ spectra of these polymers to conduct the end-group analysis, as explained in Section II of the Supporting Information. Even though that was not possible, it is expected that the SBC-based TPHUs have comparable molecular weights to those of the MBC-based TPHUs because polymerization was conducted in a solvent for 24 h.

While examining the microstructure of the sugar-based TPHUs, the WAXS spectra of Figure S5 showed differences in the diffraction angles that depended on the choice of the diamine ($12^\circ/21^\circ/23^\circ/24^\circ$ and $7^\circ/20^\circ/23^\circ$ for the HMDA and DAD-based TPHUs, respectively). It seems that the choice of the isomeric dicarbonate did not affect the microstructure of the TPHUs on the WAXS scale with the calculated crystallinities of 76 and 77% for the SBC and MBC-based TPHUs, respectively, from powder XRD. The crystalline domains were expected to be dominant because the TPHUs were very brittle and crumbly. Besides, the SAXS analysis in Figure 2 revealed nanophase separation between the sugar-derived dicarbonate units and the short-chain diamine units, which was anticipated based on similar analysis conducted on

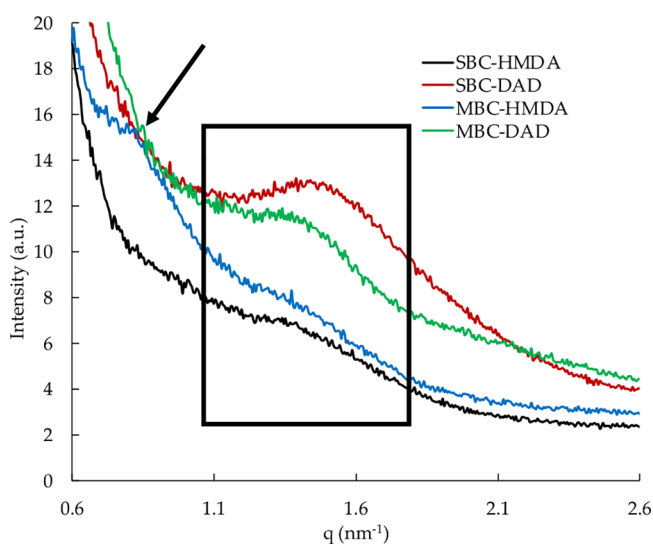


Figure 2. SAXS spectra showing nanophase separation in the microstructure of the sugar-based TPHUs. The intensity is given in the logarithmic scale.

MBC and SBC-derived hybrid PHUs.³⁰ Similar to that previous study, the interdomain spacing, d , of the MBC-based TPHUs were higher than those of the SBC-based TPHUs, with MBC-HMDA showing a hexagonal $p6mm$ spacial geometry-like ($1, \sqrt{3}...$) while the other TPHUs had randomly ordered chains.

The nanophase separation in the sugar-based TPHUs was also obvious from the thermal properties presented in Table 2 and Figure S6. The TGA traces of Figure S6 exhibited two distinct degradation steps; the first one corresponding to the amine soft segments (35–40 wt%) and the second one to the carbonate hard segments of the urethane linkages, as previously explained on the thermal degradation of conventional TPHUs and observed in similar SBC-based PHU systems.^{29,57,58} Regardless of the isomeric sugar-derived dicarbonate or diamine used, the TPHUs showed similar thermal stability with similar 10 and 50% degradation temperatures, $T_{d,10\%}$ and $T_{d,50\%}$ respectively, presented in Table 2. Only MBC-HMDA had a higher $T_{d,10\%}$ by 15 $^\circ\text{C}$ and that could be due to its chain ordering, as previously explained. The DSC results provided interesting characteristics of the TPHUs under study. First, all the TPHUs exhibited melting points (even though those of the HMDA-based TPHUs were low in intensity and broad), which indicated the presence of crystalline domains. In contrast, the DAD-based TPHUs presented two melting points at ~ 100 and 140 $^\circ\text{C}$, which reveal two types of crystalline clusters or segregation between hard and soft segments, which is more probable. This aspect was observed in other PHUs studied by Lamarzelle et al.^{36,59} and by Magliozzi et al., who observed crystallization and two melting points when analyzing their PHU prepared from DAD.¹⁷ Moreover, the melting enthalpy of SBC-DAD was higher than that of MBC-DAD, which is in correlation with the higher melting point of SBC. However, although SBC has a higher melting temperature and thermal stability than MBC, their resulting polymers exhibited similar thermal stability and melting temperatures. However, the glass transition temperatures, T_g , of the SBC-based TPHUs were 7 $^\circ\text{C}$ higher than those of the MBC-based TPHUs. The difference is not significant as it fades when using soft segments of higher molecular weights like it was previously done,³⁰ but it is notable that the furan ring of SBC provides less flexibility to the TPHU chain. Also, the furan ring in SBC and MBC provides less flexibility to the polymeric chains when compared to a TPHU prepared from the linear aliphatic erythritol dicarbonate and HMDA under similar conditions ($T_g = 9$ $^\circ\text{C}$).³¹ Going from the shorter HMDA to the longer DAD increased the chain flexibility such that the T_g increased by 10 $^\circ\text{C}$, which was expected.

The rheological behavior of the sugar-based TPHUs were also examined to unveil any effect that SBC and MBC have on the TPHUs properties. From the amplitude sweeps conducted at room temperature (~ 22 $^\circ\text{C}$), it was concluded that all the TPHUs have similar storage (G') and loss (G'') moduli. They exhibited a solid-like behavior with their G' higher than G'' , as presented in Figure 3. However, the dynamic mechanical thermal analysis of the TPHUs showed interesting features when measuring G' presented in Figure S7. While the DAD-based TPHUs had a decreasing trend with three different steps starting right after the melting points of these TPHUs, measured from DSC and summarized in Table 2, the HMDA-based TPHUs had a decreasing trend in G' until their melting points were reached, after which their G' started increasing. At

Table 2. Thermal Properties of the Bio-Based TPHUs

| TPHU | $T_{d,10\%}$ (°C) | $T_{d,50\%}$ (°C) | T_g (°C) | T_m (°C) ^a | ΔH_m (J/g) ^a |
|----------|-------------------|-------------------|------------|-------------------------|---------------------------------|
| SBC-HMDA | 227 | 331 | 31 | 96 | 1.62 |
| SBC-DAD | 222 | 337 | 21 | 102/138 | 7.39/8.77 |
| MBC-HMDA | 240 | 337 | 24 | 88 | 2.15 |
| MBC-DAD | 222 | 337 | 14 | 96/138 | 4.75/5.70 |
| DGC-DAD | 249 | 338 | 10 | 71/93 | 6.72/0.96 |

^aThe melting points and enthalpies of the MBC-based TPHUs were low in intensity and broad, so they were quantified approximatively.

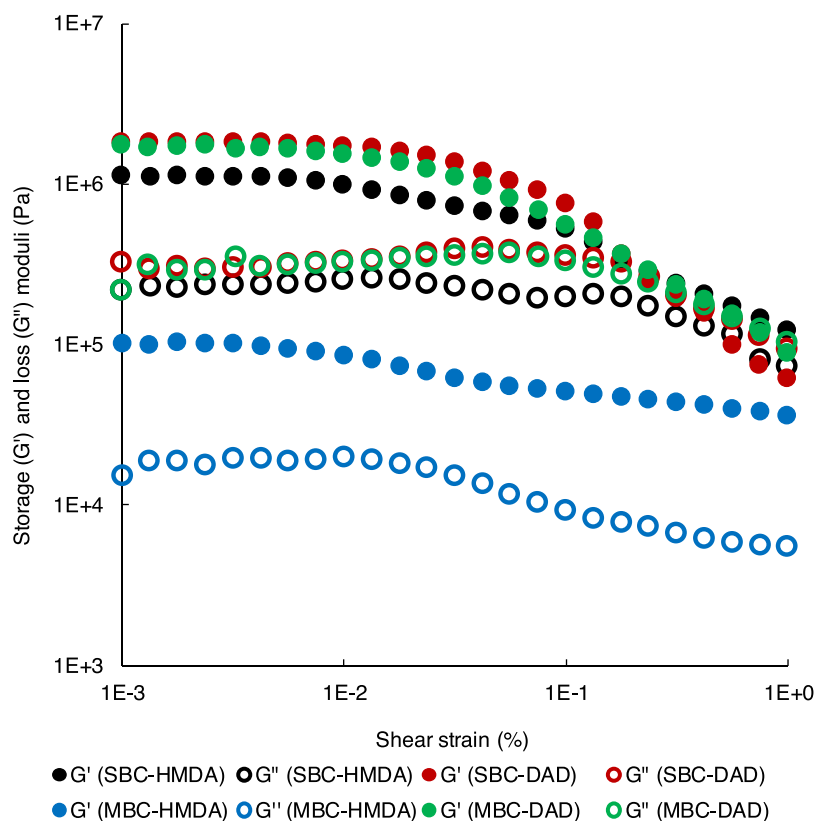


Figure 3. Amplitude sweep results conducted on the sugar-based TPHUs at room temperature (~ 22 °C) and 1 Hz.

the end of the analysis, the melted disk samples of the former lost their original shape (Figure S7), whereas those of the latter maintained their disklike shape (Figure 4). The behavior exhibited by the HMDA-based TPHUs was similar to liquid-crystals polymers (LCPs) studied by Pakula and Zentel, who observed that the mechanical properties of LCPs increase when they transition from the nematic to the isotropic phase, and that was observed at high temperatures.⁶⁰ In the case at hand, the mesogens are made of the furan rings of the hard segments, and the networks consist of the intermolecular hydrogen bonding exhibited between the amide, carbonyl, and hydroxyl groups of the hydroxyurethane linkages. The mesophase state, the intermediate state between the liquid and the solid, occurred at the melting point of these TPHUs, measured from DSC. These melting points were broad and of low intensity, which agrees with the macromolecular orientation phenomena occurring in LCPs. Indeed, at those “apparent” melting points, the chains of the HMDA-based TPHUs are re-oriented and re-ordered, and that was observed from the SAXS data measured after the polymers were heated and cooled (Figure S8). At that stage, SBC-HMDA did not show any nanophase separation, whereas MBC-HMDA exhibited a higher interdomain spacing of 8.61 nm. This

chain re-orientation in the mesophase state created self-reinforcing properties of the HMDA-based TPHUs, which was observed in Figure 5, in which the G' curves (G' in Figure S9) remained unchanged when conducting the amplitude sweeps at room temperature (~ 22 °C) and at 150 °C. In fact, different crystalline polymer systems had similar behaviors as these TPHUs, and they conserved a constant G' at temperatures as high as 200 °C.^{61–63}

Going back briefly to the main objective of this work, it is observed that the isomeric dicarbonates do not greatly affect their respective TPHUs as most properties were similar. The next section discusses the effects exhibited by replacing the more rigid sugar-based dicarbonates with the linear aliphatic DGC.

Comparison between Sugar and DGC-Based TPHUs.

To remove any variability induced by the difference in the melting points of the cyclic dicarbonates, DGC was reacted with DAD at the same conditions as SBC and MBC with DAD. Like the sugar-based TPHUs, the FT-IR spectrum of DGC-DAD in Figure S10 shows the carbonyl stretch of the formed urethane linkage at 1685 cm^{-1} . Only one stretch is present because DGC is a symmetrical cyclic dicarbonate, unlike SBC and MBC, leading to two different forms of the urethane

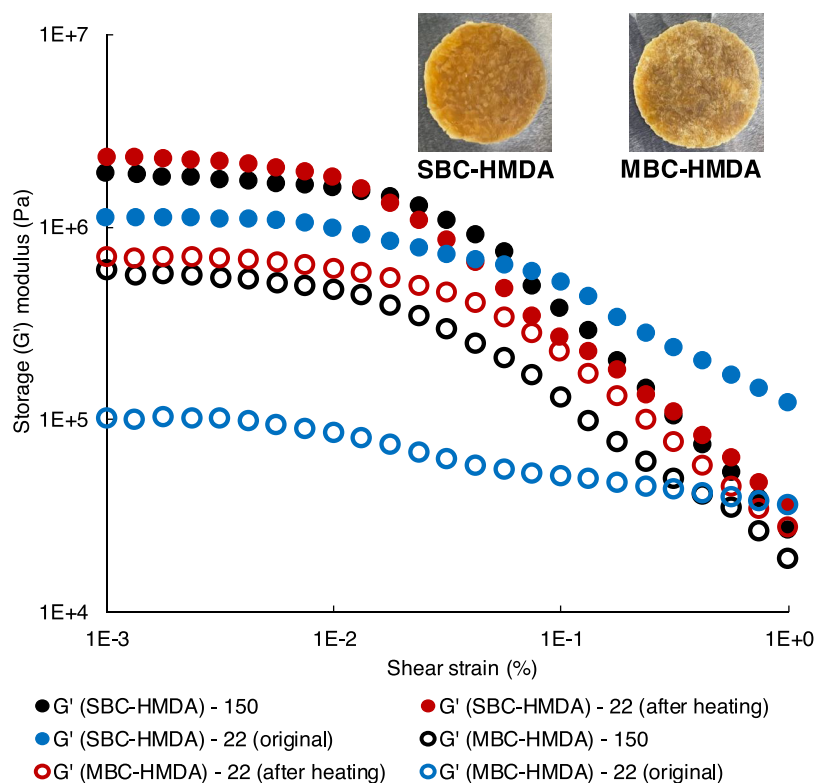


Figure 4. Storage moduli (G') of the amplitude sweep experiments conducted on SBC-HMDA and MBC-HMDA (before and after heating) at room temperature ($\sim 22^\circ\text{C}$) and 150°C with a frequency of 1 Hz. The pictures of the samples are given after heating and cooling them.

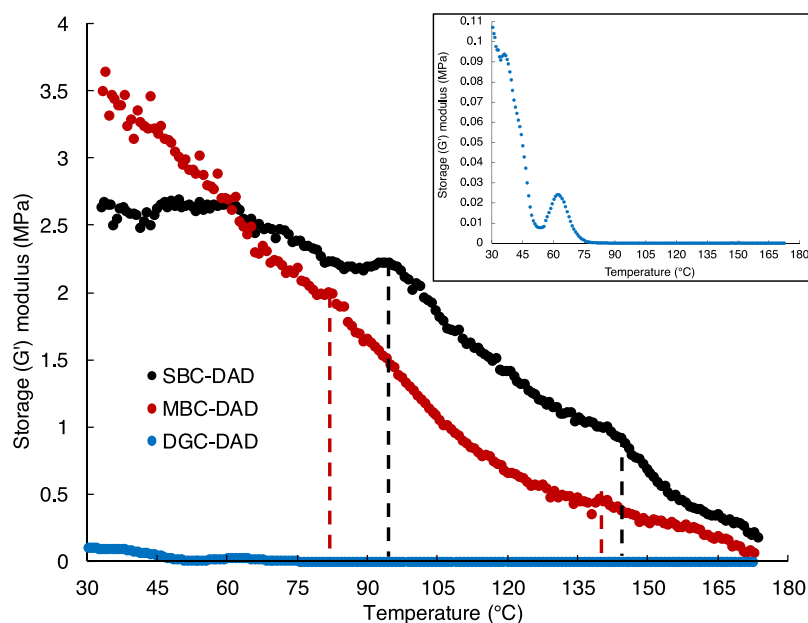


Figure 5. Storage moduli (G') of SBC-DAD, MBC-DAD, and DGC-DAD sugar-based TPHUs collected from dynamic thermal mechanical analysis conducted at a frequency of 1 Hz and 0.001% shear strain. The onset gives a closer look to the curve of DGC-DAD.

segments when the carbonate ring opens. Also, similar structural assessments were conducted from $^1\text{H-NMR}$, and the results are summarized in Table 1 with details provided in the $^1\text{H-NMR}$ subsection of Section III of the Supporting Information (Figure S11). The calculated parameters in Table 1 reveal comparable p , M_n , and D to those found for the MBC-based TPHUs, and the secOH/primOH complies with values reported for similar DGC-based TPHUs.¹³ Moreover,

replacing the sugar-based dicarbonates with DGC had a mild effect on the final TPHU microstructure, and it seems that the diffraction angles are mostly dictated by the choice of the diamine. Only the first diffraction peak of the WAXS spectrum of DGC-DAD, presented in Figure S12, appeared at 4.5° instead of 7° while the remaining peaks appeared at similar angles as the WAXS spectra of SBC or MBC-DAD. Interestingly, the SAXS measurement showed randomly

Table 3. TPHUs and PLA Estimated Solubility Parameters from the Hoftyzer–Van Krevelen Group Contribution Method

| PLA or TPHU | δ_d (MJ/m ³) ^{1/2} | δ_p (MJ/m ³) ^{1/2} | δ_h (MJ/m ³) ^{1/2} | δ (MJ/m ³) ^{1/2} | RED ^a |
|-------------|--|--|--|--|------------------|
| PLA | 15.3 | 8.4 | 11.0 | 20.6 | |
| MBC-HMDA | 16.0 | 4.3 | 15.7 | 22.9 | 0.6 |
| MBC-DAD | 17.3 | 3.7 | 14.6 | 22.9 | 0.7 |
| DGC-DAD | 18.5 | 3.7 | 14.5 | 23.8 | 0.8 |

^aThe relative energy difference, RED, was calculated between the TPHU and PLA using eq (S17) in the Supporting Information. These parameters were used to calculate the RED of the blends made of 20 wt% TPHUs and 80 wt% PLA (details are given in Section IV of the Supporting Information).

Table 4. Thermal Properties of PLA and the Blends of PLA and TPHUs (80/20 wt%/wt%)

| PLA or blends | T_{max} (°C) | T_g (°C) ^a | T_g^{est} (°C) ^b | ΔH_c (J/g) ^a | T_c (°C) ^a | ΔH_m (J/g) ^a | T_m (°C) ^a |
|------------------|----------------|-------------------------|-------------------------------|---------------------------------|-------------------------|---------------------------------|-------------------------|
| PLA ^c | 368 | 59 | | 18.71 | 123 | 17.10 | 151 |
| PLA/MBC-HMDA | 297 | 53 | 51/52 | 26.13 | 112 | 22.88 | 144/152 |
| PLA/MBC-DAD | 271 | 50 | 49/50 | 25.52 | 105 | 21.72 | 141/150 |
| PLA/DGC-DAD | 299 | 4/55 | 48/49 | 24.13 | 115 | 21.64 | 69/148 |

^aThe DSC results are based on the average of three runs. The three runs reproduced similar thermal transition properties of the blends with standard deviations varying between ± 0.4 °C and ± 1.3 °C. The value of ΔH_m was reported for both melting points of MBC-HMDA and MBC-DAD as they overlapped; however, that of DGC-DAD was reported solely for the second melting point, as ΔH_m of the first one was small with a value of 0.94 J/g. ^bThe estimated T_g s and T_g^{est} were calculated from the Flory-Fox equation and the mixing rule equations using the T_g s of PLA and the TPHUs (Fox/Mixing). The latter can be found in Table 2. ^cPLA was extruded at similar conditions to those of the blends (150 °C and 30 rpm).

ordered chains of DGC-DAD with d of 2 nm (Figure S13), which is lower than the values calculated for the sugar-based TPHU analogs, and it was also observed elsewhere.³⁰ It looks like the linear aliphatic structure of DGC leads to lower interdomain spacing than the more rigid MBC and SBC structure having a furan ring in the middle. The lack of that furan ring in DGC might also be the reason for the lower quantified crystallinity of DGC-DAD (70%) with respect to 76 and 77% of SBC-DAD and MBC-DAD, respectively. The crystallinity and interdomain spacing of DGC-DAD are given in Table 1.

Seeing that DGC did not affect the nanophase separation of the TPHUs as much as the sugar-derived dicarbonates, the TGA trace of DGC-DAD did not show two distinct steps, as shown in Figure S14. It was rather an apparent one step decrease which followed the same trend as the traces of the sugar-based TPHUs while giving close $T_{d,10\%}$ and $T_{d,50\%}$. Its $T_{d,10\%}$ was higher because DGC and DAD mix well together (lower interdomain spacing) allowing more interactions between the segments which gives better thermal stability, as observed in previously studied segmented DGC-based TPHUs.²⁵ In addition, DGC-DAD showed two melting points that were lower than those of SBC/MBC-DAD, which is in agreement with the low melting point of DGC. Even the total melting enthalpy of the former is lower than the latter one, and DGC-DAD exhibited a crystallization transition upon heating with a crystallization temperature, T_c , of 53 °C and a crystallization enthalpy, ΔH_c , of 5.83 J/g, a behavior was also observed elsewhere.²⁵ Lastly, because DGC is a linear dicarbonate, the T_g of DGC-DAD was lower than those of SBC/MBC-DAD synthesized with the more rigid dicarbonates, as observed from Table 2.

Lastly, amplitude sweep measurements conducted on DGC-DAD showed G' and G'' values ten-fold lower than those of SBC and MBC-DAD, as presented in Figure S15. This was anticipated as the furan ring in SBC and MBC stiffens the TPHU's structure. The DMTA response corresponded to the thermal behavior of DGC-DAD observed from DSC, with a sharp decrease in the storage modulus, then a small increase at

the crystallization transition because of chain reordering, after which G' kept decreasing at the melting points of the TPHU. A comparison of the DMTA between DGC-DAD, SBC-DAD, and MBC-DAD is given in Figure 5, and the different transitions were marked.

In summary, it was observed that changing the structure of the dicarbonate hard segment greatly affects the properties of the TPHUs. Next, some of these TPHUs were blended with PLA to complement our earlier study that will anticipate constructing general guidelines when blending TPHU additives into different polymer systems.²⁵

Characterization of PLA Blends with Bio-Based TPHUs. Because there was no difference between the sugar-based TPHUs based on the previous section's findings, MBC-HMDA and MBC-DAD were only blended with PLA and given their lower T_g with respect to their SBC analogs, they would be more effective at plasticizing or toughening. DGC-DAD was also studied in the blends to assess the effect of having a softer hard segment (compared to SBC or MBC) on the final blend properties. To predict the miscibility of the blends, the Hoftyzer–Van Krevelen group contribution method was used to estimate the Hansen solubility parameters of PLA and the TPHUs.²⁵ These parameters consist of three different components: dispersive forces (δ_d), polar forces (δ_p), and hydrogen bonding (δ_h), leading to the combined solubility parameter of the three (δ) and the estimation of the relative energy difference, RED, of the blends. Briefly, an RED lower than unity means a given blend is miscible. It can be seen from Table 3 (and Section IV of the Supporting Information) that by using the shorter chain diamines, the δ_d became lower while δ_p and δ_h became higher compared to the values calculated elsewhere for the DGC-based PHU prepared with longer chain diamines of oily and nonpolar Priamine 1074 and poly-(dimethylsiloxane) diamine.²⁵ This was expected because the hydroxyl group concentration increases when the urethane linkage (hard and soft segments) molecular weight decreases, so that the hydrogen bonding effects and the polarity of the TPHU chains become more significant. Hence, the calculated RED values were lower than 1, which means that the blends of

PLA with these new TPHUs were predicted to be miscible, unlike the previous ones reported.²⁵

The miscibility of the blends was also confirmed by performing TGA and DSC. In effect, the TGA traces of the blends, presented in Figure S16, followed the same trend as that of neat PLA. The derivatives of these TGA curves (wt% with respect to temperature in Figure S17) show only one maximum like PLA, which means that the blend's components burn as one constituent rather than degrading in multiple steps like in immiscible or partially immiscible blends.⁶⁴ However, the TPHUs decreased the thermal stability of PLA, whose maximum temperature, T_{max} calculated from the derivative curves of Figure S17, decreased by almost 100 °C when blending it with MBC-DAD, as observed from Table 4. Indeed, the TPHU's thermal stability, summarized in Table 2, is lower than that of PLA, so it is not surprising that the blends degrade at lower temperatures compared to PLA. Also, the TPHUs plasticized the PLA matrix by decreasing its T_g , so they altered the chain entanglements around PLA. Interestingly, PLA/MBC-HMDA and PLA/MBC-DAD blends presented one T_g that corresponds to the estimated T_g values, T_g^{est} , of these blends from the Flory-Fox and the mixing rule equations, as presented in Table 4. Therefore, these two blends are indeed miscible, as previously discussed. Nevertheless, two T_g s were measured for PLA/DGC-DAD, which might be an indication of a partially miscible blend. In general, two T_g s are observed in partially miscible blends, with one that increased from its original value and the other that decreased to satisfy the mixing rule, but that is not the case here. In fact, both T_g s of that blend decreased from their original values by 5 °C, so it seems that its components acted as plasticizers to one another. DGC-DAD has a lower G' at the extrusion temperature (150 °C) compared to those of SBC/MBC-DAD (Figure 5), and thus, it should be softer; it was dispersed in the PLA matrix into smaller droplets that are not rigid enough to plasticize PLA. This agrees with an earlier study reporting that TPUs and TPHUs with higher hard segment contents plasticized PLA because they are more rigid (in contrast to softer TPUs and TPHUs that acted more like rubber tougheners for PLA).^{25,50} It was also observed from the DGC traces that T_c of PLA decreased by 20 °C when blended, and two T_m s were observed with the lower one corresponding to the TPHUs and the second one to PLA (~150 °C), which did not change. Lastly, the crystallinity of PLA and the blends was negligible because ΔH_c was higher than ΔH_m ; therefore, these materials were considered amorphous.

To confirm that the dispersion size and rigidity of the TPHUs in the PLA matrix are the main factors responsible for plasticizing the PLA matrix, SEM images were taken after the removal of the TPHU phase from the fractured surfaces of the blends. The SEM images shown in Figure 6 compare, at 100× magnification, the surfaces of the blends with those of PLA (Figure 6A) taken as a reference. Interestingly, droplets of MBC-HMDA and MBC-DAD can be seen dispersed in the PLA matrix even at low magnifications (Figure 6B,C). They exhibit a range of different droplet sizes, but their droplets are larger than those of the DGC-DAD dispersed phase, as seen from Figure 6D. In fact, those droplets cannot be easily discerned from Figure 6D; hence, the magnification was increased to 1000× to detect them and to get a clear estimate of the droplets size, and the images are summarized in Figure S18. TPHU droplet sizes as high as 40 μm were observed for PLA/MBC-HMDA, 25 μm for PLA/MBC-DAD, and 5 μm for

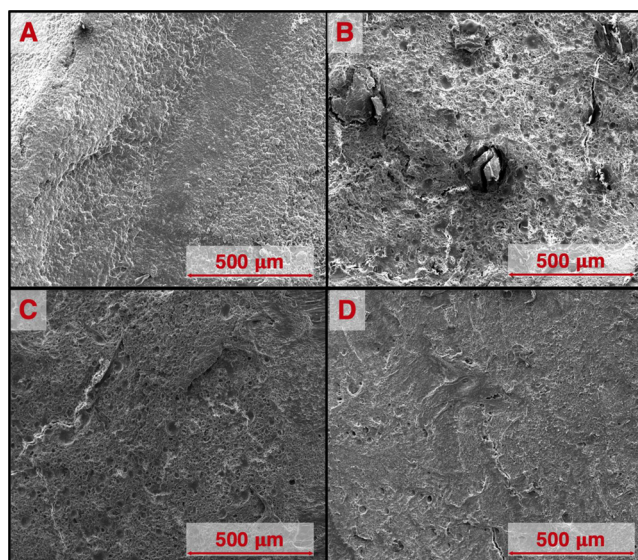


Figure 6. SEM of cryogenically fractured surfaces of (A) PLA, (B) PLA/MBC-HMDA, (C) PLA/MBC-DAD, and (D) PLA-DGC-DAD treated with DMSO to remove the TPHU phase solely (100× magnification).

PLA/DGC-DAD. It is obvious how the rheological behavior of each of the TPHUs, at the extrusion temperature, affected its mixing and dispersion in PLA. MBC-HMDA exhibiting a self-reinforcing behavior after 100 °C, like LCPs, had the biggest droplet size, followed by MBC-DAD, containing the rigid furan ring in its structure, and then the softer DGC-DAD, which exhibited the smallest droplets. However, it is interesting that even though the blends are miscible, the TPHUs tended to agglomerate in the PLA matrix as droplets which can be due to their highly crystalline nature and high hydrogen bonding interactions pre-existing between their own chains. In fact from Table 3, δ_{hs} of the TPHUs were higher than δ_h of PLA, and to further prove that observation, FTIR was conducted on the blends to assess the carbonyl stretch region of PLA, as that stretch becomes broad when hydrogen bonding interactions exist between the carbonyl groups of PLA and the hydroxyl groups of the second blend component.⁶⁵ For the blends studied herein, the carbonyl stretch of PLA was intact, which confirms the conclusions drawn in this section about the miscibility of the blends and the agglomerations of the TPHUs in the matrix of their host. The blends are miscible because of structural similarity (Table 3), but simultaneously, the TPHUs tend to aggregate because their chains exhibit high hydrogen bonding interactions with one another. This result is somewhat different from what was expected, as the blends of this work were thought to be compatible through hydrogen bonding interactions between the TPHUs and PLA, similar to Lin et al.'s work in which their hyperbranched poly(ester amide)/PLA blends (20/80 wt%/wt%) were found to be only compatible by exhibiting significant hydrogen bonding interactions between their components.⁶⁵ Thus, although the Hoftzyer–Van Krevelen group contribution method proved to give reliable predictions of the miscibility of polymer blends, this study reveals some of its limitations in blends containing TPHUs, such as DGC-DAD, as it does not account for the high crystallinity of these polymers nor for the hydrogen bonding effects exhibited between their chains.

Based on the previous observations and our previous work on blending TPHUs with PLA, the following section provides some tips on designing TPHU additives for different polymeric matrices.

Insights into Designing TPHU Additives. Because TPHUs of high molecular weights are not easily obtained, these materials can be suitable as additives, such as plasticizers, toughening agents, reinforcing agents, composites, and so forth, to different polymer systems if they are appropriately designed. First, we applied the Hoftzyer–Van Krevelen group contribution method and found it to be reliable when predicting the Hansen solubility parameters of the TPHUs and their miscibility with PLA.²⁵ Hence, this contribution method can be extended to estimate the solubility parameters of any TPHUs, synthesized from any cyclic dicarbonates and diamines, and blended with any polymer matrix. If it is used as a basis, one can predict if the designed TPHU is going to be miscible with the targeted polymer, with some limitations.

Besides, the choice of the hard and soft segments, as well as their ratios, greatly affect the thermal and rheological properties of the resulting TPHUs and their end-application. Rigid TPHUs, with higher hard segment content or made from short cyclic dicarbonates and diamines, act as reinforcing agents to their host polymer matrix. TPHUs with longer soft and hard segments are rubbery-like and can serve as plasticizers or toughening agents to the polymers they are blended with. The functional groups in both the cyclic dicarbonates and diamines also play a major role in dictating the effects the TPHUs will have on the final blends, and that is partially accounted for when conducting the group contribution analysis in the first step of the process.

As for the hydroxyl groups of the TPHUs, they are known to exhibit hydrogen bonding effects between the polymer chains. The intensity of these interactions can be decreased when using longer hard and soft segments, as previously observed, so that those hydroxyl groups interact with the host polymer matrix.²⁵ Otherwise and as observed from this study, the TPHUs will coalesce and form droplets in their host polymer matrix even if the latter possesses functional groups that can interact with the hydroxyl groups of the former.

CONCLUSIONS

Different objectives were targeted in this study. First, the differences that the isomeric sugar-derived dicarbonates, SBC and MBC, bring into the TPHU properties were examined. For that purpose, short-chain diamines, HMDA and DAD, were used in the solution polyaddition with SBC and MBC. Regardless of the dicarbonate used, the resulting TPHU properties revealed similar structural, microstructural, and rheological properties. While the thermal stability was similar, the thermal transitions revealed lower T_g s and ΔH_m s of the MBC-based TPHUs. Interestingly, MBC was more reactive than SBC with amines at room temperature, and the HMDA-based TPHUs exhibited a liquid-crystalline behavior when heated to temperatures above their apparent T_m s.

In the second phase of this study, the more rigid SBC and MBC, having furan rings in their structure, were replaced by the nonfuran containing DGC, which is a linear aliphatic dicarbonate, and the final properties of their TPHUs were assessed. DAD was used as the diamine in this case. DGC-DAD presented lower nanophase separation (d), crystallinity (X), and thermal transitions (T_g and ΔH_m). Most importantly, rheological properties were quite different compared to SBC/

MBC-DAD. DGC-DAD storage modulus was ten-fold lower compared to SBC/MBC-DAD, but its thermal stability was like them. Hence, the choice of the dicarbonate did have a measurable impact on the TPHU properties.

In the last and most important stage, seeing that there were no major differences observed between the SBC and the MBC-based TPHUs, only MBC-HMDA and MBC-DAD were selected with DGC-DAD to be blended with PLA at a composition of 20/80 wt%/wt%. The Hoftzyer–Van Krevelen group contribution method was used to estimate the solubility parameters of the TPHUs and PLA, and it predicted blend miscibility ($RED < 1$). Miscibility was tested by conducting TGA and DSC, from which the blends were observed to thermally degrade as one compound, similar to a neat PLA sample, and one T_g was measured for PLA/MBC-HMDA and PLA/MBC-DAD, respectively. PLA/DGC-DAD presented two T_g s that were shifted downward with respect to the neat homopolymers, so PLA and DGC-DAD acted as plasticizers to one another. This phenomenon was caused by the low storage modulus of DGC-DAD at the extrusion temperature of 150 °C, and smaller size droplets of DGC-DAD in the PLA matrix were observed from SEM. Coupling the SEM with FT-IR analysis, it suggests that the TPHUs exhibited high self-hydrogen bonding interactions that, even though they were predicted to be miscible with PLA, they agglomerated into sizable droplets dispersed in the matrix.

Finally, this study outlines the possible design of TPHU additives to suit different polymer matrices, which opens up guidelines toward using these materials in industrial applications such as plasticizers, reinforcing agents, rubber tougheners, and composites.

ASSOCIATED CONTENT

Supporting Information

The Supporting Information is available free of charge at <https://pubs.acs.org/doi/10.1021/acsapm.2c00673>.

TGA traces of the cyclic dicarbonates, FT-IR and ¹H-NMR of sugar-based TPHUs, WAXS, and TGA traces of sugar-based TPHUs, rheology of sugar-based TPHUs, FT-IR and ¹H-NMR of DAD-based TPHUs, WAXS and SAXS spectra, TGA traces, and rheology of DAD-based TPHUs, group contribution method and estimation of PLA and TPHUs solubility parameters and miscibility analysis of PLA/TPHU blends (RED calculations), TGA traces of the blends, and SEM images of the blends (PDF)

AUTHOR INFORMATION

Corresponding Author

Milan Marić – Department of Chemical Engineering, McGill University, Montreal, QC H3A 0C5, Canada; orcid.org/0000-0002-4984-8761; Email: milan.maric@mcgill.ca

Authors

Georges R. Younes – Department of Chemical Engineering, McGill University, Montreal, QC H3A 0C5, Canada

Marc Kamel – Department of Mechanical Engineering, American University of Beirut, Riad El-Solh/Beirut 1107 2020, Lebanon

Hatem M. Titi – Department of Chemistry, McGill University, Montreal, QC H3A 0C5, Canada; orcid.org/0000-0002-0654-1292

Mohammad Farkhondehnia – Department of Chemical Engineering, McGill University, Montreal, QC H3A 0C5, Canada

Complete contact information is available at:
<https://pubs.acs.org/10.1021/acsapm.2c00673>

Author Contributions

The manuscript was written through contributions of all authors. All authors have given approval to the final version of the manuscript.

Funding

This work was funded by the National Sciences and Engineering Research Council of Canada-Collaborative Research and Development Grants (CRDPJ 522280-17 with ADFAST Corp.), the Fonds de Recherche du Québec - Nature et Technologie, which granted Georges R. Younes a Doctorate Scholarship administered under the B2X program, and the McGill Engineering Doctoral Award was granted to Mohammad Farkhondehnia.

Notes

The authors declare no competing financial interest.

ACKNOWLEDGMENTS

The authors would like to thank the McGill Chemistry Material Characterization facility for assistance and use of their facility. The operation of MC2 and their staff are supported by the Quebec Center for Advanced Materials (QCAM).

REFERENCES

- (1) Kathalewar, M. S.; Joshi, P. B.; Sabnis, A. S.; Malshe, V. C. Non-isocyanate polyurethanes: from chemistry to applications. *RSC Adv.* **2013**, *3*, 4110–4129.
- (2) Cornille, A.; Auvergne, R.; Figovsky, O.; Boutevin, B.; Caillol, S. A perspective approach to sustainable routes for non-isocyanate polyurethanes. *Eur. Polym. J.* **2017**, *87*, 535–552.
- (3) Kreye, O.; Mutlu, H.; Meier, M. A. R. Sustainable routes to polyurethane precursors. *Green Chem.* **2013**, *15*, 1431–1455.
- (4) Nohra, B.; Candy, L.; Blanco, J. F.; Guerin, C.; Raoul, Y.; Mouloungui, Z. From Petrochemical Polyurethanes to Biobased Polyhydroxyurethanes. *Macromolecules* **2013**, *46*, 3771–3792.
- (5) Błażek, K.; Datta, J. Renewable natural resources as green alternative substrates to obtain bio-based non-isocyanate polyurethanes-review. *Crit. Rev. Environ. Sci. Technol.* **2019**, *49*, 173–211.
- (6) Carre, C.; Ecochard, Y.; Caillol, S.; Averous, L. From the Synthesis of Biobased Cyclic Carbonate to Polyhydroxyurethanes: A Promising Route towards Renewable Non-Isocyanate Polyurethanes. *ChemSusChem* **2019**, *12*, 3410–3430.
- (7) Ghasemlou, M.; Daver, F.; Ivanova, E. P.; Adhikari, B. Bio-based routes to synthesize cyclic carbonates and polyamines precursors of non-isocyanate polyurethanes: A review. *Eur. Polym. J.* **2019**, *118*, 668–684.
- (8) Meier, M. A. R. Plant-Oil-Based Polyamides and Polyurethanes: Toward Sustainable Nitrogen-Containing Thermoplastic Materials. *Macromol. Rapid Commun.* **2019**, *40*, No. 1800524.
- (9) Błażek, K.; Kasprzyk, P.; Datta, J. Diamine derivatives of dimerized fatty acids and bio-based polyether polyol as sustainable platforms for the synthesis of non-isocyanate polyurethanes. *Polymer* **2020**, *205*, No. 122768.
- (10) Froidevaux, V.; Negrell, C.; Caillol, S.; Pascault, J. P.; Boutevin, B. Biobased Amines: From Synthesis to Polymers; Present and Future. *Chem. Rev.* **2016**, *116*, 14181–14224.
- (11) Bobbink, F. D.; van Muyden, A. P.; Dyson, P. J. En route to CO₂-containing renewable materials: catalytic synthesis of polycarbonates and non-isocyanate polyhydroxyurethanes derived from cyclic carbonates. *Chem. Commun.* **2019**, *55*, 1360–1373.
- (12) Tryznowski, M.; Swiderska, A.; Zolek-Tryznowska, Z.; Golofit, T.; Parzuchowski, P. G. Facile route to multigram synthesis of environmentally friendly non-isocyanate polyurethanes. *Polymer* **2015**, *80*, 228–236.
- (13) van Velthoven, J. L. J.; Gootjes, L.; van Es, D. S.; Noorderover, B. A. J.; Meuldijk, J. Poly(hydroxy urethane)s based on renewable diglycerol dicarbonate. *Eur. Polym. J.* **2015**, *70*, 125–135.
- (14) Bossion, A.; Aguirresarobe, R. H.; Irusta, L.; Taton, D.; Cramail, H.; Grau, E.; Mecerreyes, D.; Su, C.; Liu, G. M.; Muller, A. J.; Sardon, H. Unexpected Synthesis of Segmented Poly(hydroxyurea-urethane)s from Dicyclic Carbonates and Diamines by Organocatalysis. *Macromolecules* **2018**, *51*, 5556–5566.
- (15) Tryznowski, M.; Swiderska, A. Novel high reactive bifunctional five- and six-membered bicyclic dicarbonate - synthesis and characterisation. *RSC Adv.* **2018**, *8*, 11749–11753.
- (16) Bossion, A.; Olazabal, I.; Aguirresarobe, R. H.; Marina, S.; Martín, J.; Irusta, L.; Taton, D.; Sardon, H. Synthesis of self-healable waterborne isocyanate-free poly(hydroxyurethane)-based supramolecular networks by ionic interactions. *Polym. Chem.* **2019**, *10*, 2723–2733.
- (17) Magliozzi, F.; Chollet, G.; Grau, E.; Cramail, H. Benefit of the Reactive Extrusion in the Course of Polyhydroxyurethanes Synthesis by Aminolysis of Cyclic Carbonates. *ACS Sustainable Chem. Eng.* **2019**, *7*, 17282–17292.
- (18) Peixoto, C.; Soares, A. M. S.; Araujo, A.; Olsen, B. D.; Machado, A. V. Non-isocyanate urethane linkage formation using l-lysine residues as amine sources. *Amino Acids* **2019**, *51*, 1323–1335.
- (19) Magliozzi, F.; Scali, A.; Chollet, G.; Montarnal, D.; Grau, E.; Cramail, H. Hydrolyzable Biobased Polyhydroxyurethane Networks with Shape Memory Behavior at Body Temperature. *ACS Sustainable Chem. Eng.* **2020**, *8*, 9125–9135.
- (20) Wang, D.; Chen, S.; Zhao, J.; Zhang, Z. Synthesis and characterization of self-healing cross-linked non-isocyanate polyurethanes based on Diels-Alder reaction with unsaturated polyester. *Mater. Today Commun.* **2020**, *23*, No. 101138.
- (21) Younes, G. R.; Price, G.; Dandurand, Y.; Maric, M. Study of Moisture-Curable Hybrid NIPUs Based on Glycerol with Various Diamines: Emergent Advantages of PDMS Diamines. *ACS Omega* **2020**, *5*, 30657–30670.
- (22) Zhang, C.; Wang, H.; Zhou, Q. Waterborne isocyanate-free polyurethane epoxy hybrid coatings synthesized from sustainable fatty acid diamine. *Green Chem.* **2020**, *22*, 1329–1337.
- (23) Pronoitis, C.; Hakkarainen, M.; Odelius, K. Solubility-governed architectural design of polyhydroxyurethane-graft-poly(ϵ -caprolactone) copolymers. *Polym. Chem.* **2021**, *12*, 196–208.
- (24) Younes, G. R.; Maric, M. Increasing the Hydrophobicity of Hybrid Poly(propylene glycol)-Based Polyhydroxyurethanes by Capping with Hydrophobic Diamine. *Ind. Eng. Chem. Res.* **2021**, *60*, 8159–8171.
- (25) Younes, G. R.; Marić, M. Bio-based Thermoplastic Polyhydroxyurethanes Synthesized from the Terpolymerization of a Dicarbonate and Two Diamines: Design, Rheology, and Application in Melt Blending. *Macromolecules* **2021**, *54*, 10189–10202.
- (26) Bowman, L. P.; Younes, G. R.; Marić, M. Effects of Poly(propylene glycol)-Based Triamine on the Sol/Gel Curing and Properties of Hybrid Non-Isocyanate Polyurethanes. *Macromol. React. Eng.* **2022**, *16*, No. 210055.
- (27) Mazurek-Budzyska, M. M.; Rokicki, G.; Drzewicz, M.; Guka, P. A.; Zachara, J. Bis(cyclic carbonate) based on D-mannitol, D-sorbitol and di(trimethylolpropane) in the synthesis of non-isocyanate poly(carbonate-urethane)s. *Eur. Polym. J.* **2016**, *84*, 799–811.
- (28) Clark, J. H.; Farmer, T. J.; Ingram, I. D. V.; Lie, Y.; North, M. Renewable Self-Blowing Non-Isocyanate Polyurethane Foams from Lysine and Sorbitol. *Eur. J. Org. Chem.* **2018**, *2018*, 4265–4271.
- (29) Furtwengler, P.; Averous, L. From D-sorbitol to five-membered bis(cyclo-carbonate) as a platform molecule for the synthesis of different original biobased chemicals and polymers. *Sci. Rep.* **2018**, *8*, 9134.

- (30) Younes, G. R.; Maric, M. Moisture Curable Hybrid Polyhydroxyurethanes from Sugar-Derived Dicarboxates. *Macromol. Mater. Eng.* **2021**, *306*, No. 2000715.
- (31) Schmidt, S.; Gatti, F. J.; Luitz, M.; Ritter, B. S.; Bruchmann, B.; Mulhaupt, R. Erythritol Dicarboxate as Intermediate for Solvent- and Isocyanate-Free Tailoring of Bio-Based Polyhydroxyurethane Thermoplastics and Thermoplastic Elastomers. *Macromolecules* **2017**, *50*, 2296–2303.
- (32) Poussard, L.; Mariage, J.; Grignard, B.; Detrembleur, C.; Jérôme, C.; Calberg, C.; Heinrichs, B.; De Winter, J.; Gerbaux, P.; Raquez, J. M.; Bonnaud, L.; Dubois, P. Non-Isocyanate Polyurethanes from Carbonated Soybean Oil Using Monomeric or Oligomeric Diamines To Achieve Thermosets or Thermoplastics. *Macromolecules* **2016**, *49*, 2162–2171.
- (33) Carre, C.; Bonnet, L.; Averous, L. Solvent- and catalyst-free synthesis of fully biobased nonisocyanate polyurethanes with different macromolecular architectures. *RSC Adv.* **2015**, *5*, 100390–100400.
- (34) Menard, R.; Caillol, S.; Allais, F. Chemo-Enzymatic Synthesis and Characterization of Renewable Thermoplastic and Thermoset Isocyanate-Free Poly(hydroxy)urethanes from Ferulic Acid Derivatives. *ACS Sustainable Chem.* **2017**, *5*, 1446–1456.
- (35) Maisonneuve, L.; More, A. S.; Foltran, S.; Alfos, C.; Robert, F.; Landais, Y.; Tassaing, T.; Grau, E.; Cramail, H. Novel green fatty acid-based bis-cyclic carbonates for the synthesis of isocyanate-free poly(hydroxyurethane amide)s. *RSC Adv.* **2014**, *4*, 25795–25803.
- (36) Lamarzelle, O.; Hibert, G.; Lecommandoux, S.; Grau, E.; Cramail, H. A thioglycerol route to bio-based bis-cyclic carbonates: poly(hydroxyurethane) preparation and post-functionalization. *Polym. Chem.* **2017**, *8*, 3438–3447.
- (37) Duval, C.; Kebir, N.; Charvet, A.; Martin, A.; Burel, F. Synthesis and Properties of Renewable Nonisocyanate Polyurethanes (NIPUs) from Dimethylcarbonate. *J. Polym. Sci., Part A: Polym. Chem.* **2015**, *53*, 1351–1359.
- (38) Carré, C.; Zoccheddu, H.; Delalande, S.; Pichon, P.; Avérous, L. Synthesis and characterization of advanced biobased thermoplastic nonisocyanate polyurethanes, with controlled aromatic-aliphatic architectures. *Eur. Polym. J.* **2016**, *84*, 759–769.
- (39) Beniah, G.; Chen, X.; Uno, B. E.; Liu, K.; Leitsch, E. K.; Jeon, J.; Heath, W. H.; Scheidt, K. A.; Torkelson, J. M. Combined Effects of Carbonate and Soft-Segment Molecular Structures on the Nanophase Separation and Properties of Segmented Polyhydroxyurethane. *Macromolecules* **2017**, *50*, 3193–3203.
- (40) Chen, H.; Yu, X.; Zhou, W.; Peng, S.; Zhao, X. Highly toughened polylactide (PLA) by reactive blending with novel polycaprolactone-based polyurethane (PCLU) blends. *Polym. Test.* **2018**, *70*, 275–280.
- (41) Feng, F.; Ye, L. Morphologies and mechanical properties of polylactide/thermoplastic polyurethane elastomer blends. *J. Appl. Polym. Sci.* **2011**, *119*, 2778–2783.
- (42) Feng, L.; Bian, X.; Li, G.; Chen, Z.; Chen, X. Compatibility, mechanical properties and stability of blends of polylactide and polyurethane based on poly(ethylene glycol)-b-polylactide copolymers by chain extension with diisocyanate. *Polym. Degrad. Stab.* **2016**, *125*, 148–155.
- (43) Han, J.-J.; Huang, H.-X. Preparation and characterization of biodegradable polylactide/thermoplastic polyurethane elastomer blends. *J. Appl. Polym. Sci.* **2011**, *120*, 3217–3223.
- (44) Jašo, V.; Cvetinov, M.; Rakić, S.; Petrović, Z. S. Bio-plastics and elastomers from polylactic acid/thermoplastic polyurethane blends. *J. Appl. Polym. Sci.* **2014**, *131*, 41104.
- (45) Liu, T.; Huang, R.; Qi, X.; Dong, P.; Fu, Q. Facile preparation of rapidly electro-active shape memory thermoplastic polyurethane/poly(lactide) blends via phase morphology control and incorporation of conductive fillers. *Polymer* **2017**, *114*, 28–35.
- (46) Mo, X.-Z.; Wei, F.-X.; Tan, D.-F.; Pang, J.-Y.; Lan, C.-B. The compatibilization of PLA-g-TPU graft copolymer on polylactide/thermoplastic polyurethane blends. *J. Polym. Res.* **2020**, *27*, 1–13.
- (47) Zhang, L.; Xiong, Z.; Shams, S. S.; Yu, R.; Huang, J.; Zhang, R.; Zhu, J. Free radical competitions in polylactide/bio-based thermoplastic polyurethane/free radical initiator ternary blends and their final properties. *Polymer* **2015**, *64*, 69–75.
- (48) Suthapakti, K.; Molloy, R.; Punyodom, W.; Nalampang, K.; Leejarkpai, T.; Topham, P. D.; Tighe, B. J. Biodegradable Compatibilized Poly(l-lactide)/Thermoplastic Polyurethane Blends: Design, Preparation and Property Testing. *J. Polym. Environ.* **2018**, *26*, 1818–1830.
- (49) Kahraman, Y.; Özdemir, B.; Kılıç, V.; Goksu, Y. A.; Nofar, M. Super toughened and highly ductile PLA/TPU blend systems by in situ reactive interfacial compatibilization using multifunctional epoxy-based chain extender. *J. Appl. Polym. Sci.* **2021**, *138*, 50457.
- (50) Nofar, M.; Mohammadi, M.; Carreau, P. J. Effect of TPU hard segment content on the rheological and mechanical properties of PLA/TPU blends. *J. Appl. Polym. Sci.* **2020**, *137*, 49387.
- (51) Dogan, S. K.; Reyes, E. A.; Rastogi, S.; Ozkoc, G. Reactive compatibilization of PLA/TPU blends with a diisocyanate. *J. Appl. Polym. Sci.* **2014**, *131*, 40251.
- (52) Kratochvíl, J.; Kelnar, I. Non-isothermal kinetics of cold crystallization in multicomponent PLA/thermoplastic polyurethane/nanofiller system. *J. Therm. Anal. Calorim.* **2017**, *130*, 1043–1052.
- (53) Besse, V.; Camara, F.; Mechin, F.; Fleury, E.; Caillol, S.; Pascault, J. P.; Boutevin, B. How to explain low molar masses in PolyHydroxyUrethanes (PHUs). *Eur. Polym. J.* **2015**, *71*, 1–11.
- (54) Van Krevelen, D. W.; Te Nijenhuis, K. Cohesive Properties and Solubility. In *Properties of Polymers*, 4th ed.; Elsevier: New York, 2009; pp 189–227.
- (55) Domingues, R. C. C.; Pereira, C. C.; Borges, C. P. Morphological control and properties of poly(lactic acid) hollow fibers for biomedical applications. *J. Appl. Polym. Sci.* **2017**, *134*, 45494.
- (56) Schmidt, S.; Ritter, B. S.; Kratzert, D.; Bruchmann, B.; Mulhaupt, R. Isocyanate-Free Route to Poly(carbohydrate-urethane) Thermosets and 100% Bio-Based Coatings Derived from Glycerol Feedstock. *Macromolecules* **2016**, *49*, 7268–7276.
- (57) Petrović, Z. S.; Zavargo, Z.; Flynn, J. H.; Macknight, W. J. Thermal degradation of segmented polyurethanes. *J. Appl. Polym. Sci.* **1994**, *51*, 1086–1095.
- (58) Shieh, Y. T.; Chen, H. T.; Liu, K. H.; Twu, Y. K. Thermal degradation of MDI-based segmented polyurethanes. *J. Polym. Sci., Part A: Polym. Chem.* **1999**, *37*, 4126–4134.
- (59) Lamarzelle, O.; Durand, P. L.; Wirotius, A. L.; Chollet, G.; Grau, E.; Cramail, H. Activated lipidic cyclic carbonates for non-isocyanate polyurethane synthesis. *Polym. Chem.* **2016**, *7*, 1439–1451.
- (60) Pakula, T.; Zentel, R. Mechanical behaviour of liquid-crystalline polymers and their networks. *Appl. Macromol. Chem. Phys. Angew. Makromol. Chem.* **1991**, *192*, 2401–2410.
- (61) Nakamae, K.; Nishino, T.; Ohkubo, H.; Matsuzawa, S.; Yamaura, K. Studies on the temperature dependence of the elastic modulus of crystalline regions of polymers: 14. Poly(vinyl alcohol) with different tacticities. *Polymer* **1992**, *33*, 2581–2586.
- (62) Nakamae, K.; Nishino, T.; Gotoh, Y. Temperature dependence of the elastic modulus of the crystalline regions of poly(ethylene 2,6-naphthalate). *Polymer* **1995**, *36*, 1401–1405.
- (63) Nakamae, K.; Nishino, T.; Yokoyama, F.; Matsumoto, T. Temperature dependence of the elastic modulus of crystalline regions of Poly(ethylene terephthalate). *J. Macromol. Sci., Part B: Phys.* **2007**, *27*, 407–420.
- (64) Jose, S.; Thomas, S.; Biju, P. K.; Koshy, P.; Karger-Kocsis, J. Thermal degradation and crystallisation studies of reactively compatibilised polymer blends. *Polym. Degrad. Stab.* **2008**, *93*, 1176–1187.
- (65) Lin, Y.; Zhang, K.-Y.; Dong, Z.-M.; Dong, L.-S.; Li, Y.-S. Study of Hydrogen-Bonded Blend of Polylactide with Biodegradable Hyperbranched Poly(ester amide). *Macromolecules* **2007**, *40*, 6257–6267.